Environmental Assessment and Monitoring with Image Characterization and Modeling System Using Multiscale Remote Sensing Data

NINA SIU-NGAN LAM
Department of Geography and Anthropology
Louisiana State University
Baton Rouge, Louisiana 70803

DALE QUATTROCHI
NASA
Global Hydrology and Climate Center
Marshall Space Flight Center
Huntsville, Alabama 35812

HONG-LIE QIU
Department of Geography
California State University, Los Angeles
Los Angeles, California 90032

WEI ZHAO
Department of Geography and Anthropology
Louisiana State University
Baton Rouge, Louisiana 70803

Received October 1996; accepted October 1997

With the rapid increase in spatial data, especially in the NASA–EOS (Earth Observing System) era, it is necessary to develop efficient and innovative tools to handle and analyze these data so that environmental conditions can be assessed and monitored. A main difficulty facing geographers and environmental scientists in environmental assess-

Acknowledgments: This research is supported by a research grant from NASA (Award No. NAGW-4221). We appreciate the comments of the anonymous reviewers.
Reprint requests should be directed to: Nina Siu-Ngan Lam.

CCC 1083-3404/98/020077-17

ment and measurement is that spatial analytical tools are not easily accessible. We have recently developed a remote sensing/GIS software module called ICAMS (Image Characterization And Modeling System) to provide specialized spatial analytical tools for the measurement and characterization of satellite and other forms of spatial data. ICAMS runs on both the Intergraph–MGE and the Arc/Info Unix and Windows–NT platforms. The main techniques in ICAMS include fractal measurement methods, variogram analysis, spatial autocorrelation statistics, textural measures, aggregation techniques, normalized difference vegetation index (NDVI), and delineation of land/water and vegetated/non-vegetated boundaries. In this article, we demonstrate the main applications of ICAMS on the Intergraph–MGE platform using Landsat–Thematic Mapper images from the city of Lake Charles, Louisiana. Through the availability of ICAMS to a wider scientific community, we hope to generate various studies so that improved algorithms and more reliable models for environmental assessment and monitoring can be developed.

INTRODUCTION

The use of remote sensing data in global environmental modeling studies has grown rapidly in the last decade, owing largely to the increasing availability of these and other types of spatial data in digital form at global, regional, and local scales, from many sources. The National Aeronautics and Space Administration's Earth Observing System (NASA–EOS) initiative, to be launched late in this century, will add a plethora of spatial data that will help in more effectively assessing environmental conditions and managing natural resources. The fast pace of increase in digital data, however, presents an immediate problem, that is, how these data can be handled and analyzed efficiently (Justice et al., 1995). Advances in environmental monitoring and assessment require three components. In addition to high-quality data sets, we need reliable tools to handle and analyze these data sets, and such tools must be made available to the research and policy-making communities.

The current state of environmental research recognizes that the Earth's environment is so complex that it is difficult, if not impossible, to understand all of its processes. Yet an understanding of all the processes is needed to formulate effective environmental policies. Among the problems involved in environmental modeling is that researchers are often impaired by the lack of analytical tools to analyze remote sensing data. Geographic information systems (GIS) and quantitative models offer an attractive set of techniques for environmental modeling and are increasingly recognized as a vital part of research in resource management, environmental risk assessment, and global monitoring and modeling. Integration of environmental modeling and spatial techniques is considered a top research priority, and in order to make full use of available digital data for effective environmental research the immediate need is to develop user-friendly computer systems that include useful spatial analytical functions for high-quality data (Goodchild et al., 1993).

An integral part of understanding earth processes as a system is to understand how to combine data with different spatial and temporal properties in a meaningful way. This type of multiscale data integration and modeling is a necessary component in environmental research, as environmental and ecological phenomena are scale dependent in nature. Quattrochi and Goodchild (1997) documented some of the more important scale issues in remote sensing and GIS. For example, one of the basic goals of land–atmospheric interaction modeling research is to be able to move up and down the spatial scales so that the results at one scale can be inferred to another scale (Kineman, 1993;

Steyaert, 1993; Townshend and Justice, 1988; Turner et al., 1989a, 1989b). Extrapolation of results across broad spatial scales remains the most difficult problem in global environmental research. Many methods have been suggested to tackle the scale and resolution problem. Whichever method is used, we believe that basic characterization and parameterization of image data is a prerequisite, and techniques for measuring scale effects must be developed and implemented to allow for a multiscale assessment of these data before any useful process-oriented modeling involving scale-dependent data can be made.

We have recently developed a data characterization and analysis GIS module called ICAMS (Image Characterization And Modeling System) to address two of the three following components: the research and development of innovative spatial analytical and measurement tools for characterizing multiscale remote sensing data, and the bundling of these measurement tools into an integrated, user-friendly, interactive module for easy access by the general scientific community. This article presents some of the initial results of the ICAMS project. A brief description of the design principles and functions of ICAMS, with a focus on the Intergraph–MGE platform, is first provided. Using two Landsat–Thematic Mapper (TM) images from the city of Lake Charles, Louisiana, we demonstrate the functionality of ICAMS in characterizing and measuring remote sensing images. Interpretations of the resultant indices and boundaries are presented, and suggestions are then made on how they can be used in assessing and monitoring environmental conditions.

THE ICAMS MODULE

A description of an earlier version of ICAMS on the Arc/Info platform can be found in Quattrochi, Lam, et al. (1997). In the following, we highlight the software objectives, design principles, and main functions of ICAMS, and demonstrate example applications with the use of ICAMS on the Intergraph–MGE platform. It should be noted that the same algorithms have been implemented on both Intergraph–MGE and Arc/Info platforms, but because each system has its own display and system requirements, the graphic displays and procedures to run ICAMS may be different.

Objectives and Design Principles

ICAMS is designed to provide scientists with innovative spatial analytical tools to visualize, measure, and characterize landscape patterns so that environmental conditions or processes can be assessed and monitored more effectively. In developing ICAMS, we emphasize three design elements: interactive, integrative, and innovative (the three Is). Our primary goal is to provide specialized image characterization functions, such as fractal analysis, variogram analysis, and multiscale analysis, that are not easily available in commercial GIS software. Also, we have developed ICAMS as a module compatible with the two most widely used GIS software, Intergraph–MGE and Arc/Info, instead of developing it on a generic, stand-alone platform. Also, Arc/Info has a link with another advanced image processing software—ERDAS/IMAGINE. The advantages of building a module on these two commercial GIS platforms are twofold. First, using these platforms we can utilize most of the basic image input, output, and interface functions such as file transfers, image displays, and image outputs, without the need to re-program these basic functions from ground zero. This minimizes duplication and ensures that the specialized functions in ICAMS can be made available within a shorter time frame by circumventing

extensive and time-consuming software development. Second, because these platforms have been widely used, a specialized module designed to be compatible with these systems will encourage a wider access of ICAMS.

Main Functions

ICAMS has four subsystems: image input, image output, image characterization, and specialized functions (Figure 1). The image input subsystem includes basic image processing functions, such as file transformation, georeferencing, image registration, and a variety of image viewing capabilities. The image output subsystem contains functions to output original images or derived products in two-dimensional or three-dimensional form. Moreover, the output from ICAMS (e.g., land/water boundaries) can be integrated with other forms of GIS data (e.g., economic/political boundaries) for further analysis. Most of the functions in these two subsystems already exist in Intergraph–MGE and Arc/Info. We utilize mainly their macro languages and Microsoft C++ to integrate these functions together to create the input and output subsystems in ICAMS.

In addition to providing basic descriptive statistics and histograms, the image characterization subsystem computes fractal dimensions (Lam and De Cola, 1993), variograms (Burrough, 1993; Mark and Aronson, 1984), spatial autocorrelation indices (Goodchild, 1986; Lam, Fan, and Liu, 1996), and local variance (Woodcock and Strahler, 1987). These spatial analytical tools have proved useful in the analysis of other forms of spatial data. However, their uses in characterizing remote sensing images have not been extensively employed. The availability of these functions, bundled together in an interactive GIS framework, should provide ample opportunities for the user to evaluate and explore new applications of remote sensing images using these techniques.

The specialized functions subsystem calculates the NDVI, or normalized difference vegetation index (Lillesand and Kiefer, 1994) and temperature (Lobitz, 1994; Markham and Barker, 1986), and, based on the NDVI values, the user can delineate land/water or vegetated/nonvegetated boundaries (Cherukuri, 1994). Although improved vegetation indices have been developed, such as SAVI, or Soil-Adjusted Vegetation Index, and ARVI, or Atmospherically Resistant Vegetation Index (Running, et al., 1994), NDVI is still considered important because the new indices generally require additional information that may not be available. Moreover, the U.S. EROS Data Center generates NDVI indices and maps on a regular basis.

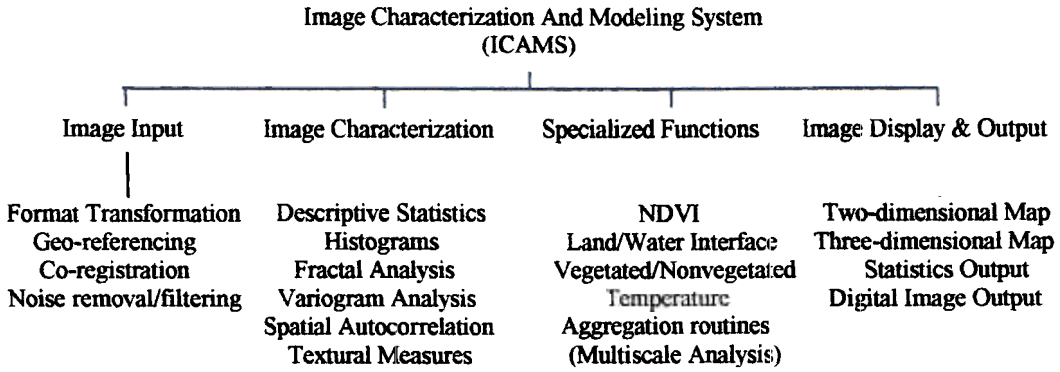

Figure 1 Main functions of ICAMS.

An aggregation function is provided to resample the image according to a filter size specified by the user. The aggregation function currently implemented is simply an averaging/smoothing function. It computes the average of all the pixels within a filter and replaces the filter with the average value. The aggregated image can be applied to the image characterization subsystem again to re-compute fractal dimensions, NDVI, or temperature, or redefine the land/water interface boundaries to evaluate the scale effects on indices and boundaries. The changes in these index values with scale (resampled image) will reveal the basic structure of the phenomena as manifested by the image and uncertainties in measurement due to scale. This information will be useful to the formulation of more accurate global environmental models, particularly those applied at multiple spatial scales.

AN APPLICATION

Study Area

Landsat–TM images acquired on two different dates from Lake Charles, Louisiana, are used to demonstrate some of the functions of ICAMS. Lake Charles had a population of about 75,000 in 1980, which decreased to 71,000 in 1992. The first image was acquired on November 30, 1984, and the second on February 8, 1993. Subsets of a 5-km × 5-km area with a pixel resolution of 25-m × 25-m were created, with each subset containing 201 × 201 pixels. Because the pixel size of the 1984 image was fixed to 25 m, the 1993 image that was provided by EOSAT at approximately 28 m was resampled to the same size, to enhance comparison. The subsets cover part of Lake Charles. The 1984 subset has been used as a representative urban landscape in a previous study that examines the fractal properties of remote sensing images (Lam, 1990). The selection of the same study area for the present study is based on the availability of data on two dates, so that analysis of temporal changes can be made. At the same time, we realize that the study area covers a medium-size urban area with little urban growth; therefore, significant changes in terms of land cover are not expected in this region between these two dates.

Figure 2 displays two images using bands 2 (blue), 3 (green), and 4 (red). Although large changes in land cover were not expected, a visual comparison between the two images shows that the 1993 image has slightly more roads and buildings, especially in the southeast corner and along the highway (Highway 210) in the southern part of the image. Table 1 lists the summary statistics of all seven bands for the two images. With the exception of the thermal band (band 6), the 1993 image generally has smaller ranges of spectral reflectance values, lower maximum values, and smaller coefficients of variation. Although these two Landsat images were not normalized to minimize sensor calibration offsets and differences in atmospheric effects [for example, using the "dark object subtraction" technique (Coppin and Bauer, 1994)], these aspatial measures of data variability can still be used and interpreted in conjunction with the spatial measures computed below.

Landscape Characterization with the Use of Fractal Indices

The fractal analysis module in ICAMS was applied to the two images to examine their spatial characteristics. The overarching question for this section of analysis is, how fractal dimensions change with spectral band, pixel resolution, and date of the image. The

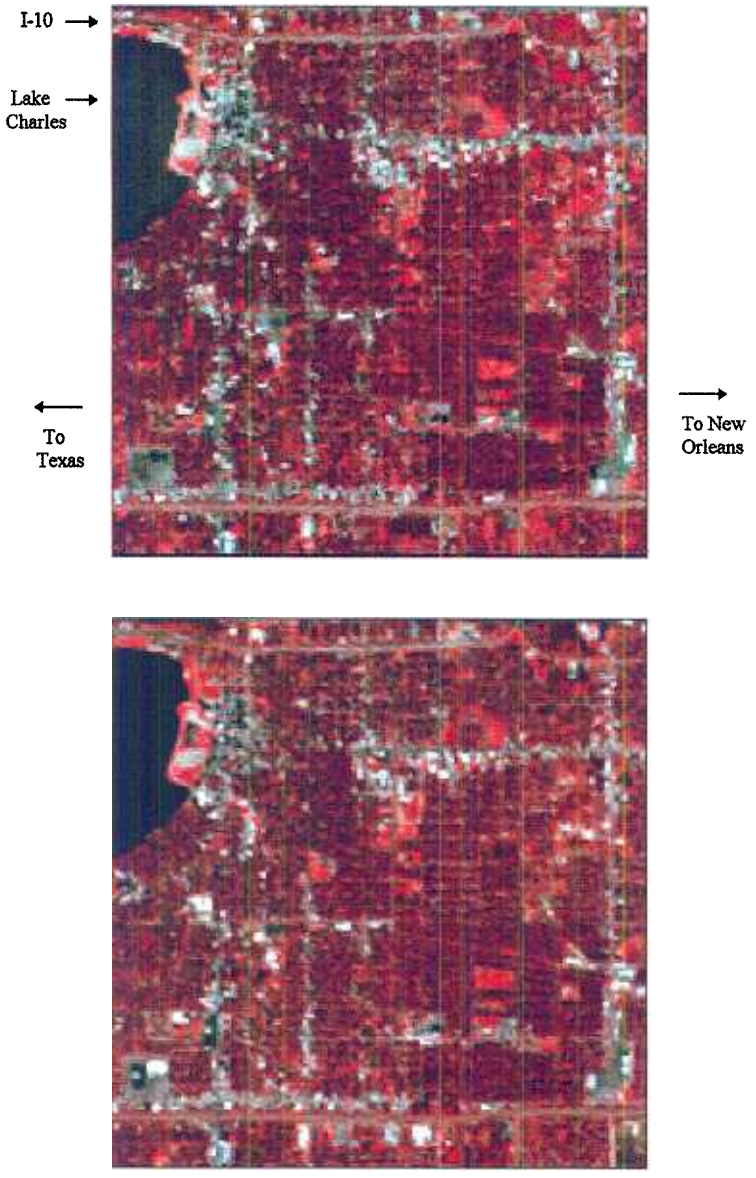

Figure 2 False color composite of the 1984 (top) and 1993 (bottom) images using bands 2 (blue), 3 (green), and 4 (red).

answer to this question, if tested with more images and analyses in the future, can be used to determine whether fractal dimension is an effective means for assessing and monitoring environmental conditions or landscape characteristics from remote sensing data.

There has been voluminous literature on the concepts and uses of fractals since Mandelbrot coined the term in 1975 (Mandelbrot, 1977, 1983). In geosciences, fractals have been used mainly for measuring and simulating spatial forms and processes, and

TABLE 1 • Summary Statistics of the Original and Resampled 1984 and 1993 Images

	Original 1984					*Original 1993*				
Band	*Min*	*Max*	*Mean*	*S.D.*	*C.V.*	*Min*	*Max*	*Mean*	*S.D.*	*C.V.*
1	40	255	70	13	0.18	35	164	59	9	0.15
2	13	126	27	8	0.28	15	84	24	5	0.22
3	8	158	31	11	0.36	13	102	27	8	0.29
4	4	138	46	12	0.26	6	91	39	9	0.23
5	0	232	52	17	0.33	0	147	51	15	0.30
6	116	146	132	4	0.03	109	140	120	3	0.02
7	0	148	22	10	0.45	0	102	24	9	0.38
	Resampled 1984					*Resampled 1993*				
Band	*Min*	*Max*	*Mean*	*S.D.*	*C.V.*	*Min*	*Max*	*Mean*	*S.D.*	*C.V.*
1	54	170	70	12	0.16	46	136	59	8	0.14
2	17	83	27	7	0.25	16	69	24	5	0.21
3	15	108	31	10	0.33	13	81	26	7	0.26
4	6	89	46	11	0.23	8	80	39	8	0.21
5	2	147	52	16	0.31	1	124	51	14	0.28
6	116	145	132	4	0.03	110	138	120	2	0.02
7	0	82	22	9	0.41	0	83	24	9	0.36

are considered an attractive spatial analytical tool (Goodchild and Mark, 1987; Lam and De Cola, 1993). Despite the numerous applications in the last two decades, there are very few direct references to the application of fractals in remote sensing (De Cola, 1989; Lam, 1990). An expanded employment of fractals in remote sensing research is considered useful to a better understanding of the relation between surface variation and spatial properties of remotely sensed data. This is especially true when one considers that remote sensing is the main source of data that we can use for analyzing the spatial dependence of surface and atmospheric phenomena at relatively large scales and over large areas (Lovejoy and Schertzer, 1988, 1990; Davis et al., 1991).

The measurement of the fractal dimension, D of a spatial phenomenon is the first step toward an understanding of spatial complexity. The higher the D, the more spatial complexity is present. The fractal dimension of a point pattern can be any value between 0 and 1; a curve, between 1 and 2; and a surface, between 2 and 3. For example, coastlines have dimension values typically approximately 1.2–1.3, and topographic surfaces around 2.2–2.3 (Mandelbrot, 1983). For spectral reflectance surfaces, such as those reflected by Landsat–TM, the fractal dimensions are much higher, approximately 2.7–2.9 (Lam, 1990; Jaggi, Quattrochi, and Lam, 1993).

There are many methods to define and measure the fractal dimensions of curves and surfaces. The following provides a brief description of how fractal dimension is calculated in ICAMS to assist interpretation of the results computed below. More detailed descriptions of the major algorithms for geoscience applications can be found in Klinkenberg and Goodchild (1992); Lam and De Cola (1993); Olsen, Ramsey, and Winn (1993); and Klinkenberg (1994).

The key concept underlying fractals is *self-similarity*. Many curves and surfaces are self-similar either strictly or statistically, meaning that the curve or surface is made up of

copies of itself in a reduced scale. The number of copies (m) and the scale reduction factor (r) can be used to determine the dimensionality of the curve or surface, where $D = -\log(m)/\log(r)$ (Falconer, 1990). Practically, the D value of a curve is estimated by measuring the length of the curve using various step sizes, a procedure commonly called the walking-divider method. The more irregular the curve, the greater increase in length as step size decreases. Such an inverse relationship between total line length and step size can be captured by a linear regression:

$$\log(L) = C + B\log(S),$$

where L is the line length, S is the step size, B is the slope of the regression, and C is the constant. D can then be calculated by

$$D = 1 - B.$$

In addition to computing R^2 for the regression, the scatter plot illustrating the relationship between step size and line length, known as the fractal plot, is often used as a visual aid to determine whether the linear fit is good for all step sizes (Figure 4). Many studies have shown that fractal plots of empirical curves are seldom linear, with many of them demonstrating an obvious break (Mark and Aronson, 1984). This indicates that real-world phenomena are seldom pure fractals and self-similarity rarely exists at all scales. In such cases, specific fractal dimensions are defined only for specific *scale ranges* at which the regression behaves linearly. Information on the fractal dimensions and their associated ranges could be utilized to explore the issue of scale and resolution (Lam and Quattrochi, 1992).

We implemented three fractal surface measurement methods in ICAMS: isarithm, variogram, and triangular prism methods. The isarithm method was used to compute the fractal dimensions of the images in this study. The isarithm method follows the walking-divider logic by measuring the dimensions of individual isarithms derived from the remote sensing surface (i.e., the iso-spectral reflectance lines). The D value is calculated using

$$D = 2 - B.$$

The final D of the surface is the average of the isarithms that have R^2 greater than 0.9. This algorithm is slightly different from the one presented in Lam's 1990 study, which averaged all isarithms regardless of the R^2 values. In ICAMS, the user has a choice of whether the calculation is based only along rows, columns, or both directions. Other user input includes the isarithm interval and number of walks. Table 2 and the corresponding Figure 3 compare the results of the two images. The number of walks were set to 6 (i.e., 1,

TABLE 2 • Fractal Dimension Values for the Original and Re-sampled (101 × 101) Images

Band	*Original 1984*	*Resampled 1984*	*Original 1993*	*Resampled 1993*
1	2.949	2.904	2.810	2.842
2	2.930	2.913	2.796	2.841
3	2.920	2.910	2.806	2.811
4	2.763	2.743	2.705	2.656
5	2.701	2.641	2.727	2.718
6	2.239	2.522	2.306	2.560
7	2.839	2.785	2.767	2.744

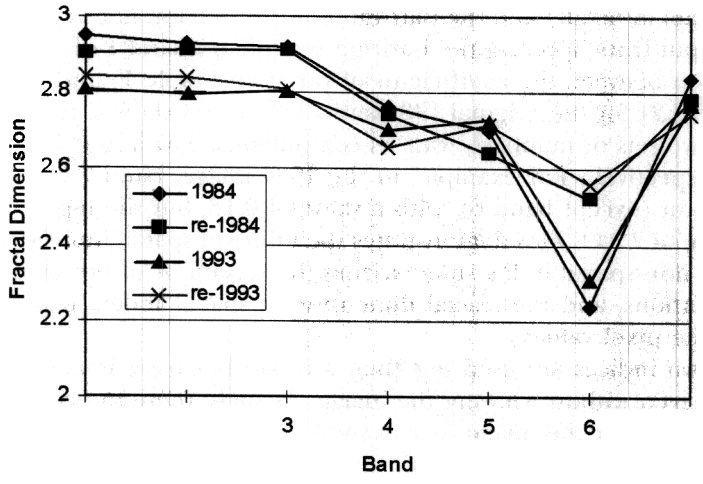

Figure 3 Plots of fractal dimension values.

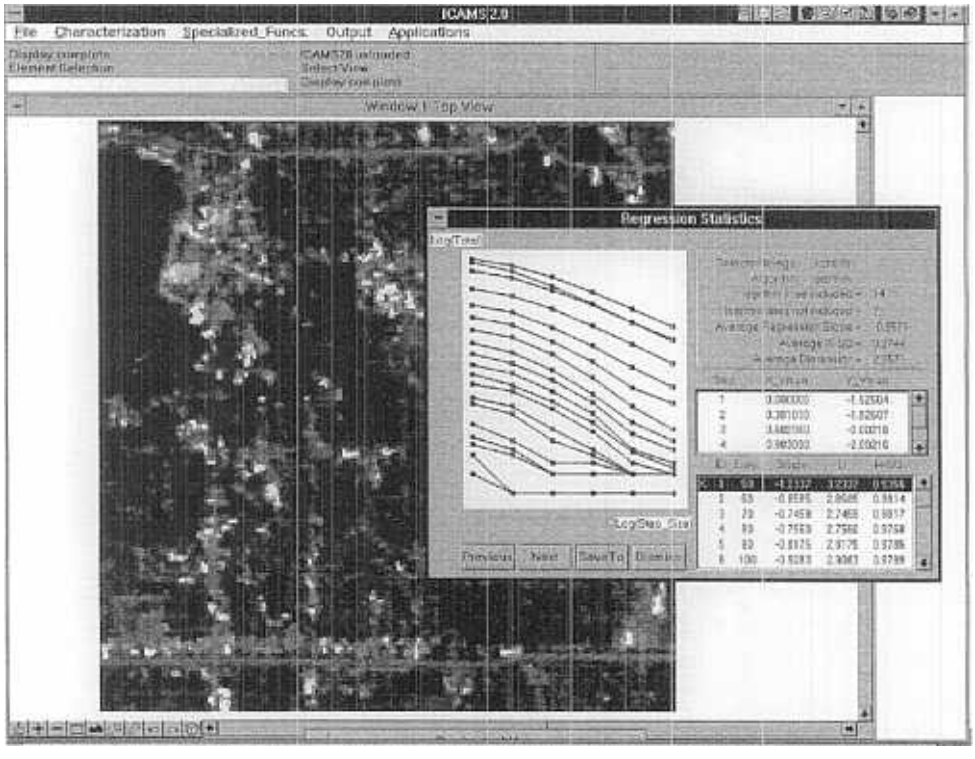

Figure 4 Example output from applying the isarithmic module with the use of Band 1 of the 1984 image.

2, 4, 8, 16, 32 pixel intervals) and the isarithm interval to 2 for all calculations. Figure 4 is an example output from applying the isarithm module on band 1 of the 1984 image.

A comparison between the coefficients of variation (Table 1) and the fractal dimension values (Table 2) for the original 1984 and 1993 images show a moderate correlation between these two sets of numbers, with r's computed as 0.67 and 0.73 for the 1984 and 1993 images, respectively. For example, in the 1984 image, band 1 has the lowest coefficient of variation (except band 6), with a value of 0.18, but the highest fractal dimension, with a value of 2.949. This demonstrates the utility of spatial indices: The coefficient of variation is a non-spatial index summarizing the variations of the pixel values regardless of their locations, and the fractal dimension, a spatial index, describes the spatial complexity of the pixel values.

When the two indices are used together, a broad but basic impression of an image can be formed, even without viewing the image. As such, these indices could be used as part of the metadata for the image. For example, when an image has a high coefficient of variation but a relatively low fractal dimension, such as band 5 of the 1984 image, the surface would most likely exhibit a more spatially homogeneous pattern, sometimes with a detectable trend (see Figure 5). On the contrary, if an image has a low coefficient of variation but high fractal dimension, such as band 1, the surface is much more frag-

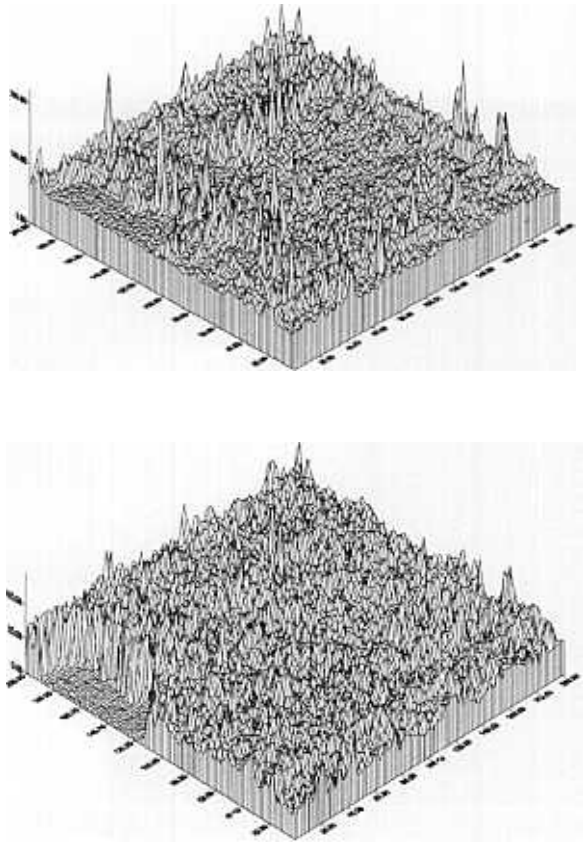

Figure 5 Three-dimensional display of band 1 (Top) and band 5 (Bottom) of the 1984 image.

mented and spatially varying. In addition to the traditional nonspatial statistics, this result confirms the need to utilize spatial indices in visualizing and detecting environmental patterns. The fractal indices used here have added information and served as a quick tool in understanding the spatial dimension of the image.

Multiscale and Multi-Temporal Assessments

To characterize the effects of pixel resolution on the computed indices, the aggregation module in ICAMS was applied with a 2 × 2 smoothing/averaging filter to aggregate the original images (201 × 201 pixels) into resampled images with 101 × 101 pixels. The resampled images were then applied to the fractal module using the same isarithm method to re-compute their fractal dimensions. The resultant fractal dimension values for the resampled images are listed in Table 2 and displayed in Figure 3. To enhance comparison, the coefficients of variation of the resampled images were also computed (see Table 1).

In a multi-scale setting, when comparing the spatial, or fractal dimension, with non-spatial, or coefficient of variation, results show that coefficients of variation and the fractal dimension values generally decrease with decreasing pixel resolution, except in band 6. The correlation coefficients between the coefficient of variation and the fractal dimension also decrease to a value close to 0.44 for both images. Band 6 exhibits a distinct reverse trend, with much higher fractal dimensions resulted in the resampled images. This can be easily explained because the original sensor resolution of band 6 that was about 120 m was artificially resampled to 25 m to conform with the rest of the bands in Landsat–TM images, resulting in a much smoother and less spatially complex surface. The 2 × 2 filter applied to this band increased the pixel resolution to 50 × 50 m and in effect reduced the smoothness, thereby resulting in a higher fractal dimension. This aspect of spatial information is not reflected by the coefficient of variation. Our findings further suggest the need for more effective spatial indices in characterizing remote sensing images.

Although the following was not tested here, if band 6 is further aggregated, the fractal dimension will continue to increase until the resolution reaches to 120 m, and thereafter, it may increase or decrease. The resolution at which the fractal dimension yields the highest value can be considered as the scale of action, the "characteristic" scale, or the optimal scale for analysis (Woodcock and Strahler, 1987). The use of fractal dimension in characterizing scale has been suggested earlier (Lam and Quattrochi, 1992). With ICAMS, it is easier to perform such analysis for a variety of images.

In terms of spectral band (see Figure 3), the results from all four images, original and resampled images of the two dates, seem to indicate three groups of spectral bands based on their similarity in fractal dimension values. Group A contains bands 1, 2, and 3 and has the highest dimensions, whereas group B contains bands 4 and 5 and has lower dimensions. Group C is band 7, which has a dimension value lying between groups A and B. As expected, fractal dimension values of the thermal band (band 6) are significantly lower, because of the smoother surfaces created from resampling from a coarser sensor resolution to a finer resolution. This suggests that the fractal dimension values computed for the spectral bands can be used as a potential guide to select certain bands for further analysis. In this case, a band from each of the three groups could be picked, instead of using all six bands, to reduce the complexity and time of analysis normally required for examining all bands. We expect that this kind of application will become

more significant and widespread when hyperspectral images such as AVIRIS (Airborne Visible InfraRed Imaging Spectrometer), which has 224 spectral bands, become available.

When the two images from two different dates are compared, Table 2 and the corresponding Figure 3 show that the 1993 image in general yields lower fractal dimensions. Because very little change occurred in Lake Charles during the 9-year period, differences in dimension values may be because of the smaller ranges of spectral reflectance and lower maximum values for all bands, except band 6 (see Table 1), rather than changes in land cover between the two dates. It is possible that normalization of the two images may reduce the differences. It is not known whether the smaller spectral ranges and lower maximum values were caused by a general deterioration of the sensor through time or a phenomenon specific to this particular TM scene. Although the computed fractal dimension values have adequately reflected the changes in spectral reflectance values, our initial multi-temporal analysis has pointed to the main difficulty in land-cover change detection, which is to distinguish real land-cover changes from spurious changes due to factors such as atmosphere, sensor, and sun angle. With ICAMS available, however, more images from different regions with similar time periods could be examined, or different techniques, such as band ratio images, could be applied to analyze further how the information on changes in index values can be used effectively in assessing the true conditions of environment.

This example has pointed to the need for two analyses in the near future. First, as noted earlier, accurate comparison of multi-date images requires more elaborate atmospheric calibration and/or normalization of the images (Jensen, 1996). Although the impact of not normalizing the images may be minimized because ratios (NDVI), instead of absolute numbers are used, in the future it would be useful to document the effects of the various algorithms on calibrated/uncalibrated or normalized/unnormalized imagery. Second, the fractal module in ICAMS mainly focuses on the computation of global indices for the entire study area. Local fractal measures, which may reflect changes in local areas more effectively, should be further explored and implemented (De Jong and Burrough, 1995; Mallat, 1989).

Delineation of Boundaries

To demonstrate the utility of ICAMS in delineating major boundaries, we applied the land/water and vegetated/non-vegetated boundary delineation modules to the two images. There are different methods to determine these boundaries, each with its own advantages and disadvantages (Cherukuri, 1994). We implemented the NDVI method to delineate these boundaries because of its reasonable accuracy, simplicity, and flexibility in allowing the user to visualize and modify the results interactively.

In delineating the boundaries, the NDVI ratio must first be computed. NDVI is a ratio between the red and infrared bands. For Landsat–TM images, NDVI is derived from using:

$$\text{NDVI} = (\text{band } 4 - \text{band } 3)/(\text{band } 4 + \text{band } 3).$$

In general, clouds, snow, water, moist soil, and bright non-vegetated surfaces have NDVI values less than zero, rock and dry bare soils have values close to zero, and positive NDVI values generally indicate vegetated areas. For example, NDVI values for the conterminous United States computed from the 1990 NOAA–AVHRR (Advanced Very High Resolution Radiometer) images have a range of 0.5 to 0.66 for vegetation (Lillesand and Kiefer, 1994). To assist the user in determining the boundaries, we set –0.1 as the default

threshold value to delineate land and water. Pixels with a value smaller than and equal to −0.1 are classified as water, whereas pixels with a value greater than −0.1 are classified as land. Similarly, a value of 0.25 was used as the default threshold value to delineate vegetated and non-vegetated boundaries. As mentioned earlier, these threshold values can be easily modified so that changes in boundaries due to threshold value changes can be visualized and evaluated. Furthermore, the output can be integrated with other data layers for further analysis.

Figure 6 shows the land/water boundaries at the two time periods using the default threshold values. Lake Charles, in the upper left corner, is clearly identified as water. The 1984 image generally has more tiny pockets of water pixels than that of the 1993 image, which could indicate misclassification. However, by changing the threshold value from the default of −0.1 to a value of −0.2, fewer water pixels were defined. In fact, the redefined boundaries on the 1984 image now resemble closely the land/water boundaries derived from using the default value on the 1993 image. Detailed research on the variability of NDVI as well as the accuracy of the default threshold values in different types of the images is out of the scope of the present article. The main point, however, is that ICAMS can be used effectively to explore further these various issues.

Figure 7 compares the vegetated/non-vegetated boundaries defined by using the same threshold value (0.25) for the two dates. The 1984 image shows slightly more vegetated areas. The roads and buildings at the southeast corner of the image, which were not in the 1984 image, were correctly identified as vegetated areas in 1984 and nonvegetated areas in 1993.

CONCLUSIONS

Using two images for Lake Charles, Louisiana, we have demonstrated how ICAMS can be applied to characterizing temporal differences in remote sensing images for environmental assessment and measurement. We have demonstrated the need for spatial indices, such as fractal dimension, in revealing the spatial characteristics of the images. Using fractal dimension with the traditional non-spatial statistics, such as coefficient of variation, a basic impression of the image can be formed even without viewing the image. These simple indices could serve as part of the metadata of the image that could then be used as a guide to search an image for rapid change detection and monitoring. This type of library application will have tremendous potential when voluminous image data are available during the NASA–EOS era. Moreover, fractal dimension values of individual bands could be utilized as a guide for selecting individual or combinations of bands for analysis. Such application will be especially useful to the analysis of hyperspectral images.

Through the multi-scale analysis, we have shown that except for band 6, fractal dimension values generally decrease with decreasing pixel resolution. The reverse trend shown in band 6 further indicates that fractal indices could be used, together with other scale methods, to identify the "characteristic" or optimal scale of analysis. Scale analysis through ICAMS, therefore, can provide a quick assessment of the scale effects on the derived indices and boundaries, thus contributing to more accurate environmental assessment and monitoring, and eventually to the development of more sensible environmental or land-use policies for a region.

The development of ICAMS is an evolving process, meaning that continuous improvement to the software will have to be made. Issues such as the reliability of the methods and the usefulness of the indices will have to be further examined. Furthermore, as

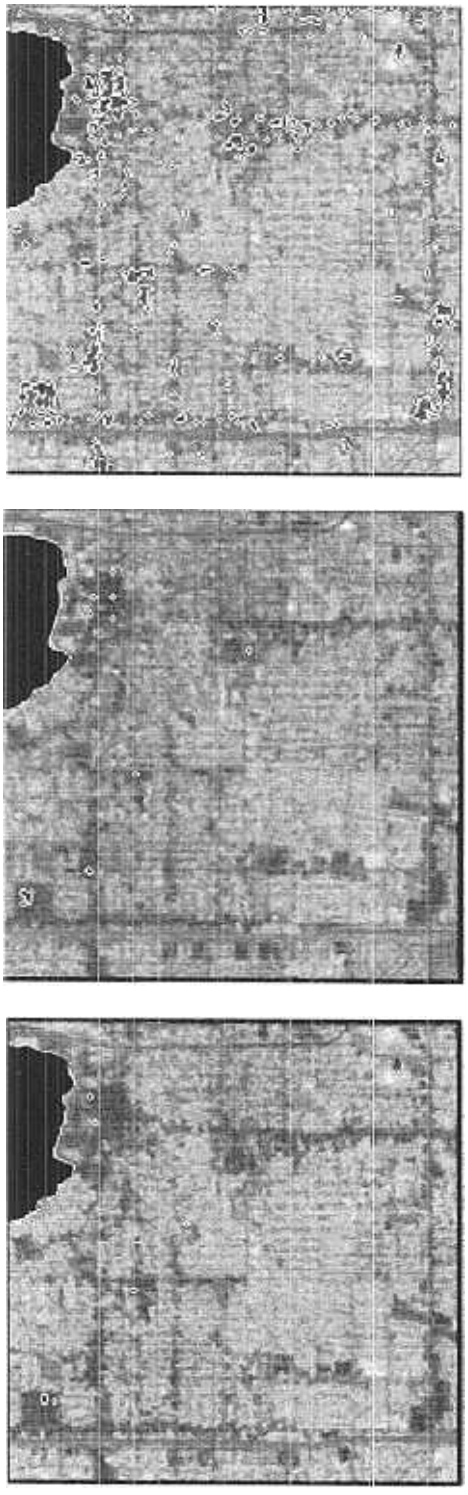

Figure 6 Land/water boundaries using a threshold value of −0.1 for the 1984 and 1993 images (top and middle) and a threshold value of −0.2 for the 1984 image (bottom).

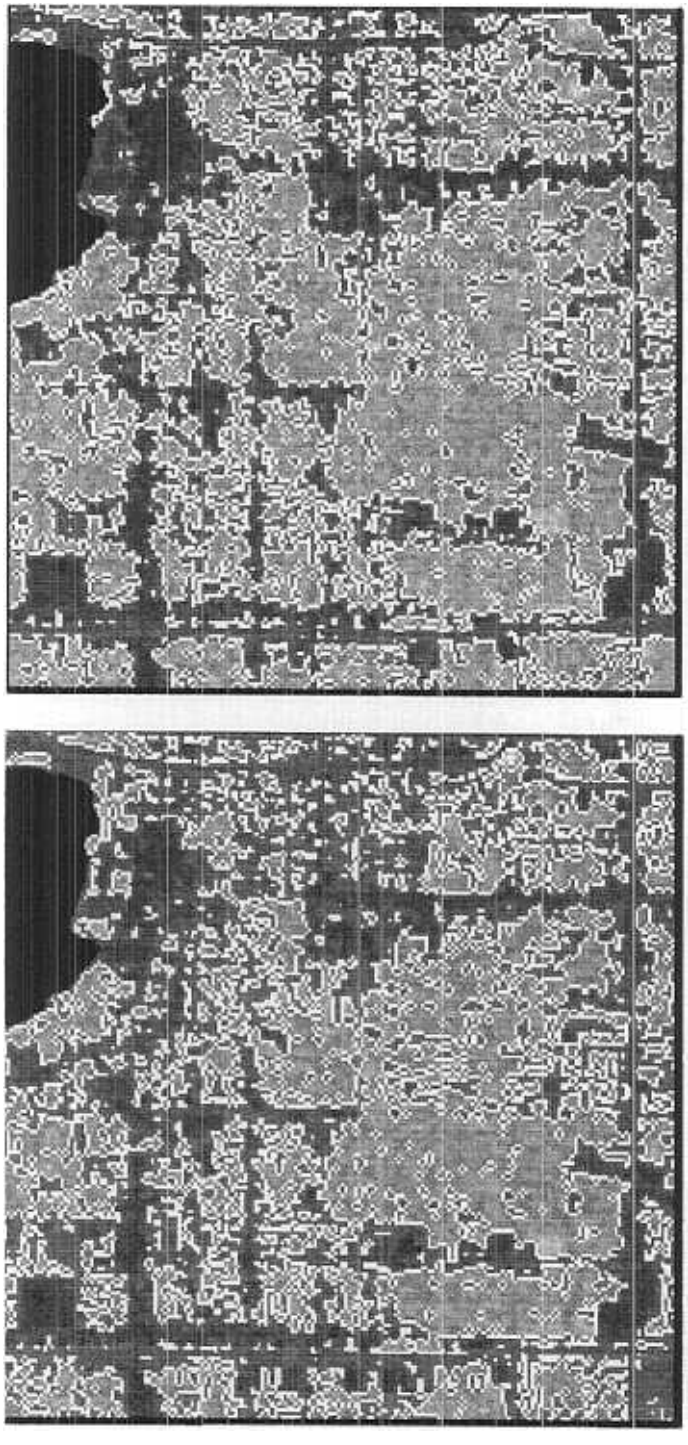

Figure 7 Vegetated and non-vegetated regions defined by the threshold value (0.25) for the 1984 (top) and 1993 (bottom) images.

hardware and software platforms, as well as data needs and data requirements change, ICAMS will have to be modified. So it can be accessed through the Internet, future improvements of ICAMS will include the development of the software on a stand-alone platform using computer languages such as JAVA. By making this software available to a wider community, we hope that improvement can be made in methods, tools, and innovative applications. Through application by a diverse user group, ICAMS can evolve from the exploratory to the operational stage as a technique for environmental assessment and policy development.

REFERENCES

Burrough, P.A. (1993). Fractals and Geostatistical Methods in Landscape Studies. *In* Lam, N.S.-N., and De Cola, L. (eds). *Fractals in Geography*, Englewood Cliffs, NJ: Prentice Hall, pp. 87–121.

Cherukuri, R. (1994). *Evaluation of Methods for the Delineation of Land/Water Interface Conditions Using AVHRR Imagery.* M.S. thesis, Department of Geography and Anthropology, Louisiana State University.

Coppin, P.R. and Bauer, M.E. (1994). Processing of Multitemporal Landsat TM Imagery to Optimize Extraction of Forest Cover Change Features. *IEEE Transactions on Geoscience and Remote Sensing* **32**(4), 918–927.

Davis, F.W., Quattrochi, D.A., Ridd, M.K., Lam, N.S.-N, Walsh, S.J., Michaelson, J.C., Franklin, J., Stow, D.A., Johannsen, C.J., and Johnston, C.A. (1991). Environmental Analysis Using Integrated GIS and Remotely Sensed Data: Some Research Needs and Priorities. *Photogrammetric Engineering and Remote Sensing* **57**, 689–697.

De Cola, L. (1989). Fractal Analysis of a Classified Landsat Scene. *Photogrammetric Engineering and Remote Sensing* **55**, 601–610.

De Jong, S.M., and Burrough, P.A. (1995). A Fractal Approach to the Classification of Mediterranean Vegetation Types in Remotely Sensed Images. *Photogrammetric Engineering and Remote Sensing* **61**(8), 1041–1053.

Falconer, K. (1990). *Fractal Geometry.* New York, NY: Wiley.

Goodchild, M.F. (1986). *Spatial Autocorrelation* [CATMOG (Concepts and Techniques in Modern Geography) 47]. Norwich, England: Geo Books.

Goodchild, M.F., and Mark, D.M. (1987). The Fractal Nature of Geographic Phenomena. *Annals of the Association of American Geographers* **77**(2), 265–278.

Goodchild, M.F., Parks, B.O., and Steyaert, L.T. (1993). *Environmental Modeling with GIS.* New York: Oxford University Press.

Jaggi, S.D., Quattrochi, D.A., and Lam, N.S.-N. (1993). Implementation and Operation of Three Fractal Measurement Algorithms for Analysis of Remote Sensing Data. *Computers and Geosciences* **19**(6), 745–767.

Jensen, J.R. (1996). *Introductory Digital Image Processing: A Remote Sensing Perspective.* Saddle River, NJ: Prentice-Hall.

Justice, C.O., Bailey, G.B., Maiden, M.E., Rasool, S.I., Strebel, D.E., and Tarpley, J.D. (1995). Recent Data and Information System Initiatives for Remotely Sensed Measurements of the Land Surface. *Remote Sensing of Environment* **51**(1), 235–244.

Kineman, J.J. (1993). What is a Scientific Database? Design Considerations for Global Characterization in the NOAA-EPA Global Ecosystems Database Project. *In* Goodchild, M.F., Parks, B.O., and Steyaert, L.T. (eds). *Environmental Modeling with GIS.* New York: Oxford University Press, pp. 372–378.

Klinkenberg, B. (1994). A Review of Methods Used to Determine the Fractal Dimension of Linear Features. *Mathematical Geology* **26**, 23–33.

Klinkenberg, B., and Goodchild, M.F. (1992). The Fractal Properties of Topography: A Comparison of Methods. *Earth Surface Processes and Landforms* **17**, 217–234.

Lam, N.S.-N. (1990). Description and Measurement of Landsat TM Image Using Fractals. *Photogrammetric Engineering and Remote Sensing* **56**, 187–195.

Lam, N.S.-N., and Quattrochi, D.A. (1992). On the Issue of Scale, Resolution, and Fractal Analysis in the Mapping Sciences. *The Professional Geographer* **44**(1), 88–98.

Lam, N.S.-N., and De Cola, L. (eds.) (1993). *Fractals in Geography.* Englewood Cliffs, NJ: Prentice Hall.

Lam, N.S.-N., Fan, M., and Liu, K.B. (1996). Spatial-Temporal Spread of the AIDS Epidemic: A Correlogram Analysis of Four Regions of the United States. *Geographical Analysis* **28**(2), 93–107.

Lillesand, T.M., and Kiefer, R.W. (1994). *Remote Sensing and Image Interpretation* (3rd ed.). New York: Wiley.

Lobitz, B. (1994). *Correlations of Vegetation with Surface Temperature in Three Louisiana Cities.* M.L.A. thesis, School of Landscape Architecture, Louisiana State University.

Lovejoy, S., and Schertzer, D. (1988). Extreme Variability, Scaling and Fractals in Remote Sensing: Analysis and Simulation. In Muller, J.P. (ed). *Digital Image Processing in Remote Sensing.* Philadelphia: Taylor & Francis, pp. 177–212.

Lovejoy, S., and Schertzer, D. (1990). Multifractals, Universality Classes and Satellite and Radar Measurements of Cloud and Rain Fields. *Journal of Geophysical Research* **95**(D3), 2021–2034.

Mallat, S.G. (1989). A Theory for Multiresolution Signal Decomposition: The Wavelet Representation. *IEEE Transactions on Pattern Analysis and Machine Intelligence* **PAM-11**(7), 674–693.

Mark, D.M., and Aronson, P.B. (1984). Scale-Dependent Fractal Dimensions of Topographic Surfaces: An Empirical Investigation, with Applications in Geomorphology and Computer Mapping. *Mathematical Geology* **11**, 671–684.

Markham, B.L., and Barker, J.L. (1986). Landsat MSS and TM Post-Calibration Dynamic Ranges, Exoatmospheric Reflectances and At-Satellite Temperatures. *EOSAT Landsat Technical Notes* **1**, 3–8.

Mandelbrot, B. (1977). *Fractals: Form, Chance and Dimension.* New York: W.H. Freeman and Co.

Mandelbrot, B. (1983). *The Fractal Geometry of Nature.* New York: W.H. Freeman and Co.

Olsen, E.R., Ramsey, R.D., and Winn, D.S. (1993). A Modified Fractal Dimension as a Measure of Landscape Diversity. *Photogrammetric Engineering and Remote Sensing* **59**(10), 1517–1520.

Quattrochi, Q.A., and Goodchild, M.F. (1997). *Scale in Remote Sensing and GIS.* Boca Raton, FL: CRC Lewis Publishers.

Quattrochi, Q.A., Lam, N.S.-N., Qiu, H.L., and Zhao, W. (1997). Image Characterization and Modeling System (ICAMS): A Geographic Information System for the Characterization and Modeling of Multi-Scale Remote Sensing Data. *In* Quattrochi, D.A., and Goodchild, M.F. (eds). *Scale in Remote Sensing and GIS.* Boca Raton, FL: CRC Lewis Publishers, pp. 295–307.

Running, S.W., Justice, C.O., Salomonson, V., et al. (1994). Terrestrial Remote Sensing and Algorithms Planned for EOS/MODIS. *International Journal of Remote Sensing* **15**(17), 3587–3620.

Steyaert, L.T. (1993). A Perspective on the State of Environmental Simulation Modeling. *In* Goodchild, M.F., Parks, B.O., and Steyaert, L.T. (eds): *Environmental Modeling with GIS.* New York: Oxford University Press, pp. 16–30.

Townshend, J.R.G., and Justice, C.O. (1988). Selecting the Spatial Resolution of Satellite Sensors Required for Global Monitoring of Land Transformations. *International Journal of Remote Sensing* **9**, 187–236.

Turner, M.G., Dale, V.H., and Gardner, R.H. (1989a). Predicting across Scales: Theory Development and Testing. *Landscape Ecology* **3**(3/4), 245–252.

Turner, M.G., O'Neill, R.V., Gardner, R.H., and Milne, B.T. (1989b). Effects of Changing Spatial Scale on the Analysis of Landscape Pattern. *Landscape Ecology* **3**(3/4), 153–162.

Woodcock, C.E., and Strahler, A.H. (1987). The Factor of Scale in Remote Sensing. *Remote Sensing of Environment* **21**, 311–332.